Solid-State NMR Detection, Characterization, and Quantification of the Multiple Aluminum Environments in US-Y Catalysts by ^{27}Al MAS and MQMAS Experiments at Very High Field

Colin A. Fyfe,*,† Jeremy L. Bretherton,† and Lau Y. Lam‡

Contribution from the Department of Chemistry, University of British Columbia, 2036 Main Mall, Vancouver, B.C., Canada V6T 1Z1, and Research Centre−CENPES, Petrobas, Cid. University Q7, Rio de Janeiro, R.J., Brazil 22280-040

Received August 29, 2000. Revised Manuscript Received November 9, 2000

Abstract: The detection of all of the aluminum present in steamed zeolite H−Y catalysts by ^{27}Al MAS NMR at 14.4 T (600 MHz for ^{1}H) and 18.8T (800 MHz for ^{1}H) is reported. Further, it is shown that it is possible by ^{27}Al MAS and MQMAS NMR measurements to clearly identify four separate aluminum environments which are characteristic of these materials and to unambiguously assign their coordinations. Average chemical shift and quadrupolar coupling parameters are used to accurately simulate the ^{27}Al MAS NMR spectra at 9.4 T (400 MHz for ^{1}H), 14.4 T (600 MHz for ^{1}H) and 18.8 T (800 MHz for ^{1}H) in terms of these four aluminum environments. In addition, these average chemical shift and quadrupolar coupling parameters are used to calculate peak positions in the ^{27}Al MQMAS isotropic dimension that are in good agreement with the experimental data acquired at 9.4 and 18.8 T.

Introduction

Zeolites are highly crystalline materials whose structures are 3-dimensional networks composed of channels and cavities of molecular dimensions built from corner and edge sharing SiO_4^{4-} and AlO_4^{5-} tetrahedra.[1] For every tetrahedral position occupied by an Al atom there must be a charge balancing cation (M^{x+}) present, leading to the general zeolite oxide formula: $M^{x+}_{n/x}[(SiO_2)_m(AlO_2)_n]\cdot yH_2O$, where $m + n = 1$.

In their acid forms, zeolites exhibit both Brønsted and Lewis acidity by which they can catalyze reactions and their structures impose molecular size and shape selectivity. Acid zeolites are formed by exchanging NH_4^+ for the charge-balancing cations (such as Na^+) which are present from the synthesis. The ammonium ions decompose above 350 °C, liberating NH_3(g) and leaving behind "H^+". Steam treatment of the resulting acid zeolites at elevated temperatures removes Al from the frameworks and yields active, "ultrastable" catalysts.[2] These are used widely in the petroleum and petrochemical industries, particularly for catalytic cracking in gasoline production.

The most widely used of these materials is ultrastable-Y (USY) formed by steam treatment of the acid form of faujasite (Figure 1), also known as zeolite HY. Early ^{29}Si MAS spectra clearly documented the increase in the framework Si/Al ratio which the steaming produced,[3−6] but in these studies the nature of the aluminum species present was much less well described, due to the relatively poor resolution of the ^{27}Al MAS spectra. This was at least in part because of the relatively low magnetic fields (≤400 MHz for protons) and spinning rates (≤4 kHz) which were available at that time. However, it was clear that six-coordinate aluminum (Al^{OCT}) was produced even under the mild conditions employed for calcination (ca. 500 °C) and that steaming generated substantial amounts of amorphous-like material, characterized by a broad resonance between the signals of the tetrahedral framework aluminum (Al^{TET}) at ≈60 ppm and Al^{OCT} at ≈0 ppm.[3−10] Various authors subsequently demonstrated that the maximum in the chemical shift for this

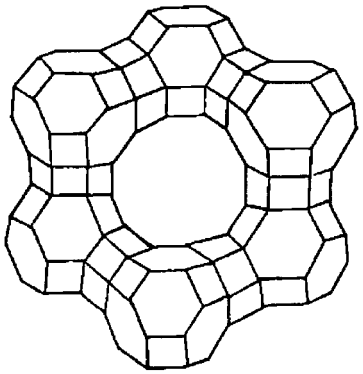

Figure 1. Schematic representation of the framework structure of Faujasite. Each line represents a T−O−T linkage (where T = Framework tetrahedral position, occupied by either silicon or aluminum atoms, located at the intersection of the lines and the oxygen atoms are not shown). For clarity, the sodalite cage in the front portion of the structure is omitted and extraframework species are not shown.

† University of British Columbia.

‡ Cid. University Q7.

(1) Meier, W. M.; Olson, D. H.; Baerlocher, C. H. *Atlas of Zeolite Structure Types*, 4th ed.; Elseiver: London, 1996.

(2) Occelli, M. L. *Fluid Catalytic Cracking II−Concepts in Catalytic Design*; ACS Symp. Ser. 452; American Chemical Society: Washington, DC, 1991; pp 27−44.

(3) Klinowski, J.; Thomas, J. M.; Fyfe, C. A.; Gobbi, G. C. *Nature* **1982**, *296*, 533−536.

(4) Scherzer, J. *Am. Chem. Soc. Symp. Ser.* **1984**, *248*, 157−200.

(5) Klinowski, J.; Fyfe, C. A.; Gobbi, G. C. *J. Chem. Soc., Faraday Trans. 1* **1985**, *81*, 3003−3019.

(6) Freude, D.; Brunner, E.; Pfeifer, H.; Prager, D.; Jerschkewitz, H.-G.; Lohse, U.; Oehlmann, G. *Chem. Phys. Lett.* **1987**, *139*, 325−330.

(7) (a) Samoson, A.; Lippmaa, E.; Engelhardt, G.; Lohse, U.; Jerschkewitz, H.-G. *Chem. Phys. Lett.* **1987**, *134*, 589−592. (b) Ray, G. J.; Samoson, A. *Zeolites* **1993**, *13*, 410−413.

10.1021/ja003210k CCC: $20.00
Published on Web 05/12/2001

resonance was similar to that of pentacoordinate aluminum Al^{PENT} and assigned the resonance to this species.[7b,8,12,13] However, other authors proposed that it was due to Al in a more distorted tetrahedral environment.[6,7,10,11] Quantitation of these spectra was also a general problem, with approximately 30% of the total aluminum known to be present not being observed (so-called "invisible aluminum"),[3,6,8−12] even when very small pulse angles were used.[7a]

More recently the availability of higher field strengths (500 MHz) and the use of nutation dependent spectroscopy[13] have provided further information on the multiple aluminum environments present. An excellent summary of this work has been given by Fripiat et al.,[13] who also drew parallels between the ^{27}Al spectra of the USY materials and those of amorphous alumina gels containing 4-, 5-, and 6-coordinate aluminum,[15,16] interpreting the ^{27}Al NMR spectra of USY in terms of these three coordinations.

The resolution of ^{27}Al MAS spectra is limited because MAS reduces but does not completely average the second-order quadrupolar interaction. There is improved resolution when satellite spectroscopy is used,[20] but again, the interaction is only reduced and not eliminated. DOR and DAS experiments[21,22] will perform this averaging but are not well-suited to these and to other systems where there is line broadening due to their amorphous nature. For example, in an application of the DOR technique to USY, Ray and Samoson[7b] obtained only a marginal gain in ^{27}Al spectral resolution. Further limitations are that in DOR experiments, the outer rotor is limited to a spinning rate of $\approx$1 kHz and the short T_1 values of ^{27}Al destroy the signal during the "storage times" required for the angle changes in DAS experiments.

However, the experiment of Multiple Quantum Magic Angle Spinning (MQMAS), recently introduced by Frydman,[14] is not limited by either slow spinning or short T_1 values and therefore provides an alternative approach to the investigation of this type of material. Further, the second-order quadrupolar interaction is inversely field dependent and experiments on quadrupolar nuclei, including MAS and MQMAS, will be much easier and in most cases have much more success at high magnetic field strengths.

In the present paper, we present the results of a detailed investigation of a representative USY material by ^{27}Al MAS and MQMAS NMR spectroscopies with fast sample spinning carried out at fields of 17.6 and 18.8 T and compare the results to those obtained at lower fields (9.4 and 14.4 T). Four well-defined ^{27}Al environments are found and quantified and their coordinations clearly defined, providing a sound basis for further investigations of the role of aluminum in these important catalytic materials. A preliminary account of this work has been published.[23]

Experimental Section

Materials. The amorphous alumina gel containing substantial amounts of 4-, 5-, and 6-coordinate aluminum was prepared exactly as described by Fripiat.[16]

The USY sample was prepared from ammonium exchanged zeolite Y, which was then steam calcined at 600 °C, ammonium exchanged, and steam calcined again at 600 °C. It had a BET area of 560 m^2/g, mesopore area of 40 m^2/g, and a micropore volume of 0.266 mL/g. IR measurements gave a framework SiO_2/Al_2O_3 ratio of 18.2/1 and the X-ray crystallinity was 110% (reference NaY sample 120%).

Equipment. Powder XRD patterns were obtained using a Seimens D5000 powder diffractometer and Cu Kα radiation. Thermogravimetric analysis (TGA) was carried out using a TG51 thermogavimetric analyzer under a flow of 80 cm^3/min of dry nitrogen gas. ^{29}Si and ^{27}Al spectra were obtained at 79.50 and 104.26 MHz, respectively, using a Bruker MSL 400 spectrometer. For ^{27}Al, the 90° solid pulse width was 1.6 μs and the spectra were referenced to 1 M aqueous $Al(NO_3)_3$ solution. For ^{29}Si, the 90° pulse width was 8.0 μs and the spectra were referenced to TMS. ^{27}Al spectra were also obtained at 156.38 (14.4 T, 600 MHz for protons), 195.40 (17.6 T, 750 MHz for protons), and 208.43 MHz (18.8 T, 800 MHz for protons). The 14.4 T spectra were recorded on a Bruker AMX 600 spectrometer and those at 17.6 and 18.8 T on Varian Inova systems to which we were granted access at the Pacific Northwest National Laboratory, Richland, Washington (see Acknowledgment). All ^{27}Al spectra were obtained using home-built MAS probes incorporating a Doty Scientific 5 mm "SuperSonic" stator assembly. The (solid) 90° pulse lengths were 2.0 (156.38 MHz) and 1.7 μs (208.43 MHz) and the spectra were referenced as above. MAS experiments were conventional and echo experiments used a rotor synchronized "90−τ−180−τ−acquire" sequence. Pulse lengths of 1.0 μs were used for the single pulse experiments and for the first pulse of the echo experiments.

^{27}Al MQMAS experiments were run at 104.26, 195.40, and 208.43 MHz. At 195.40 and 208.43 MHz, the excitation was by either a two-pulse nutation[14] or the spin-locking RIACT sequence.[24] In these two cases, the coherence selection was by phase cycling. The MQMAS experiments at 104.26 MHz used pulsed field gradients for the coherence selection.[25]

2-D spectra were sheared using a t_1-dependent phase increment following the Fourier transformation in the directly detected dimension (F2). Both the isotropic F1 axis and the position of 0 ppm with respect to the transmitter were scaled by a factor of $^{12}/_{31}$ (see Appendix of ref 18).

Results and Discussion

Figure 2 shows the ^{29}Si spectrum (79.50 MHz) of the USY material together with that for the NaY starting material. The changes in the ^{29}Si spectrum from the starting material are consistent with literature data[3−6] and the previously obtained IR data (Experimental Section) and indicate that the framework Si/Al ratio has increased from 2.6 to approximately 10/1. The

(8) Gilson, J.-P.; Edwards, G. C.; Peters, A. W.; Rajagopalan, K.; Wormsbecher, R. F.; Roberie, T. G.; Shatlock, M. P. *J. Chem. Soc., Chem. Commun.* **1987**, 91−92.

(9) Shertukde, P. V.; Hall, W. K.; Dereppe, J.-M.; Marcelin, G. *J. Catal.* **1993**, *139*, 468−481.

(10) Remy, M. J.; Stanica, D.; Poncelet, G.; Feijen, E. J. P.; Grobet, P. J.; Martens, A. J.; Jacobs, P. A. *J. Phys. Chem.* **1996**, *100*, 12440−12447.

(11) Grobet, P. J.; Geerts, H.; Tielen, M.; Martens, J. A.; Jacobs, P. A. *Studies in Surface Science and Catalysis*; Elsevier: Amsterdam, 1989; Vol. 46, pp 721−734.

(12) Coster, D.; Blumenfield, A. L.; Fripiat, J. J. *J. Phys. Chem.* **1994**, *98*, 6201−6211.

(13) Blumenfield, A. L.; Fripiat, J. J. *Top. Catal.* **1997**, *4*, 119−129.

(14) Frydman, L.; Harwood, J. S. *J. Am. Chem. Soc.* **1995**, *117*, 5367−5368.

(15) Wood, T. E.; Siedle, A. R.; Hill, J. R.; Skarjune, R. P.; Goodbrake, C. J. *Mater. Res. Symp. Proc.* **1990**, *180*, 97−115.

(16) Coster, D.; Fripiat, J. J. *Chem. Mater.* **1993**, *5*, 1204−1210.

(17) Massiot, D.; Thiele, H.; Germanus, A. Extended version of Bruker Winfit. *Bruker Rep.* **1994**, *140*, 43−46.

(18) Massiot, D.; Touzo, B.; Trumeau, D.; Coutures, J. P.; Virlet, J.; Florian, P.; Grandinetti, P. J. *Solid State NMR* **1996**, *6*, 73−83.

(19) *19.* Fitzgerald, J. J., Ed. *Solid State Spectroscopy of Inorganic Materials*; ACS Symp. Ser. 717; American Chemical Society: Washington, DC, 1998; pp 182−226.

(20) Kunath-Fandrei, G.; Bastow, T. J.; Hall, J. S.; Jager, C.; Smith, G. E. *J. Phys. Chem.* **1995**, *99*, 15138−15141.

(21) Mueller, K. T.; Sun, B. Q.; Chingas, G. C.; Zwanzinger, J. W.; Terao, T.; Pines, A. *J. Magn. Reson.* **1990**, *86*, 470−487.

(22) Samoson, A.; Lipmaa, E.; Pines, A. *Mol. Phys.* **1988**, *65*, 1013−1018.

(23) Fyfe, C. A.; Bretherton, J. L.; Lam, L. Y. *Chem. Commun.* **2000**, *17*, 1575−1576.

(24) Wu, G.; Rovnyak, D.; Griffin, R. G. *J. Am. Chem. Soc.* **1996**, *118*, 9326−9332.

(25) Fyfe, C. A.; Skibsted, J.; Grondey, H.; Meyer zu Altenschilesche, H. *Chem. Phys. Lett.* **1997**, *281*, 44−48.

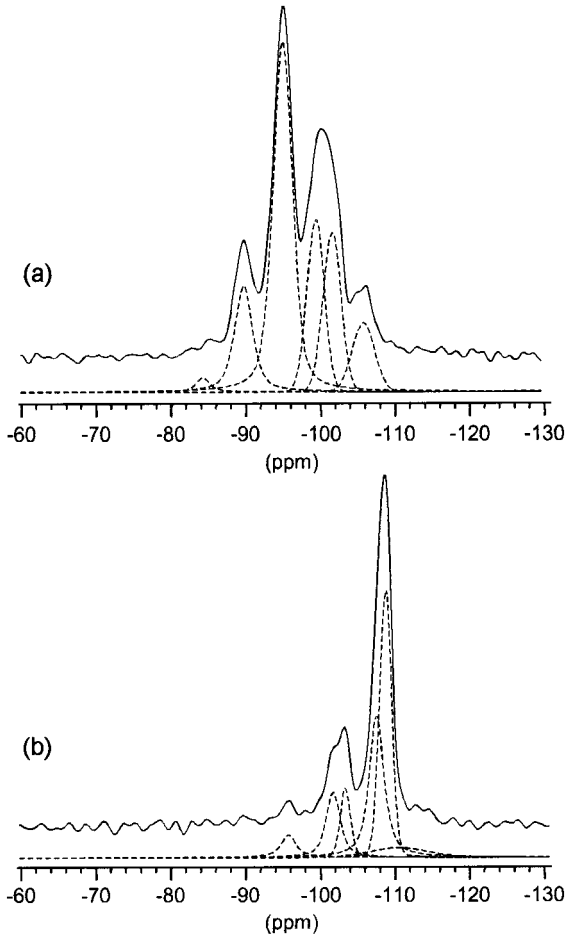

Figure 2. Single-pulse ^{29}Si MAS NMR spectra at 79.50 MHz of (a) NaY and (b) USY. (a) 2200 scans acquired using a pulse angle of 22°, a recycle delay of 10 s, and a spinning rate of 3.6 kHz. (b) 2708 scans acquired using a pulse angle of 22°, a recycle delay of 10 s, and a spinning rate of 4.1 kHz.

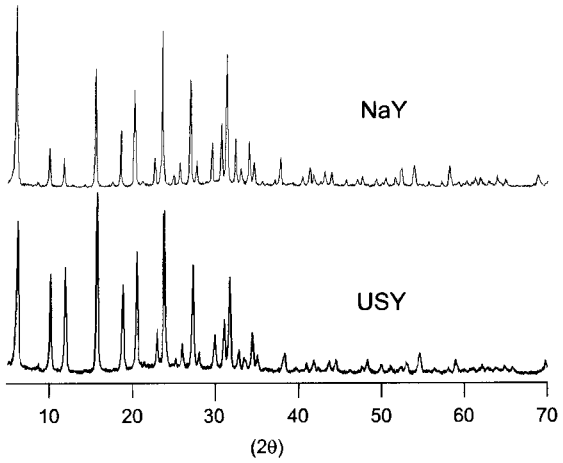

Figure 3. X-ray powder patterns of NaY and USY acquired on a Seimens D5000 powder diffractometer with Cu Kα radiation between $2\theta = 5°$ and 70° in steps of 0.025°/s.

powder XRD diffractograms (Figure 3) indicate a high framework crystallinity but also show evidence for the presence of some amorphous material of unknown composition.

Figure 4a shows the ^{27}Al single pulse MAS spectrum acquired at 104.26 MHz with spinning at 9.8 kHz. The resonances are broad and the general features of the spectrum correspond well with previous literature data at this field, indicating that the

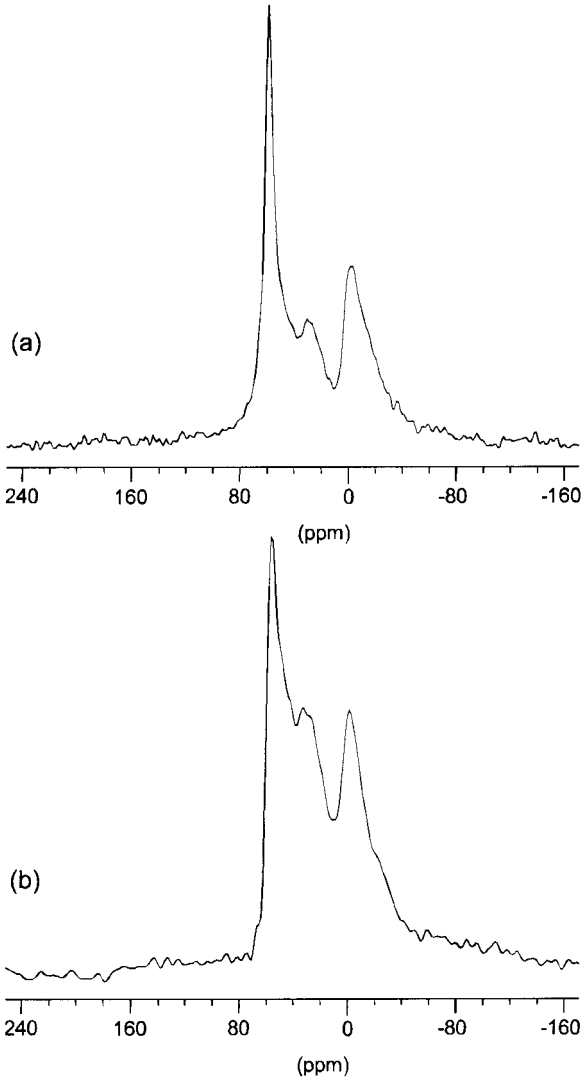

Figure 4. ^{27}Al MAS NMR spectra of USY at 104.26 MHz (a) single pulse and (b) 90−180° spin-echo. 20000 scans were acquired for each spectrum at a spinning rate of 9.8 kHz with a 200 ms recycle delay.

nature of the aluminum in the present sample is typical of this general type of catalyst. At the high spinning rate employed, there is no overlap of spinning sidebands with any of the isotropic peaks, a problem with earlier work. Three maxima are observed at 58, 30, and −3 ppm, which previous authors have assigned to 4-, 5-, and 6-coordinated aluminum species. In a recent study, Fripiat and co-workers have deconvoluted such spectra in terms of the distributions of three quadrupolar line shapes and have assigned relative intensities to the three local environments[13] discussed above, while as noted in the Introduction, other workers have assigned the same three resonances to two tetrahedral environments and one octahedral environment.[6,7,10,11]

However, even at 9.4 T, there are indications that the situation is more complex. Figure 4b shows the corresponding ^{27}Al spectrum recorded with an echo sequence. The maxima in the spectra correspond well with those of the single pulse experiments but there is an indication from the spinning sideband pattern that there is a major contribution from one or more broad resonances, centered in the isotropic pattern at approximately 30 ppm, which is greatly attenuated in the single pulse experiments. The total integrated intensities of both the single pulse and spin-echo ^{27}Al MAS spectra of weighed samples were calibrated at all fields against spectra of weighed Na-Y and Na-A

Table 1. Integrated Total Intensities of ^{27}Al MAS Spectra, Expressed as an Averaged Percentage of the Integrated Intensities of ^{27}Al MAS Spectra of Weighed Samples of Na−Y and Na-A Acquired under Identical Conditions, Adjusted for Hydration (measured by TGA) and Composition (Measured by ^{29}Si MAS NMR; See Text)

	9.4 T (±5%)	14.4 T (±10%)	18.8 T (±10%)
single pulse	65	87	95
90−180° echo	85		98

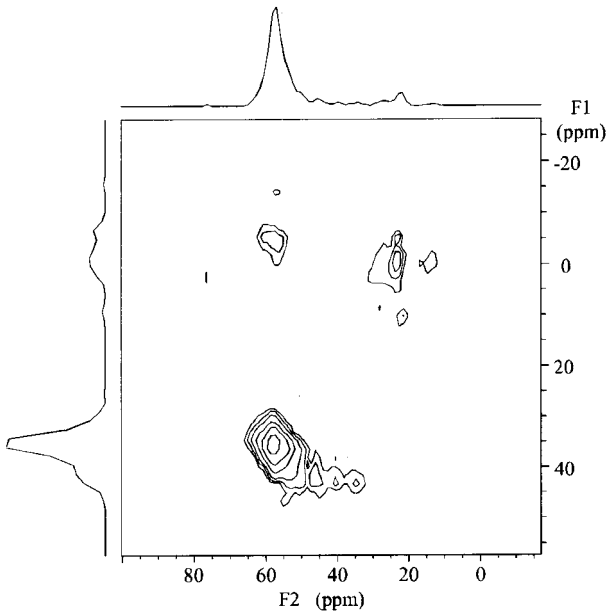

Figure 5. ^{27}Al MQMAS NMR spectrum of USY at 104.26 MHz recorded at a spinning rate of 8.7 kHz. Coherences were generated using a 3-pulse, rotationally induced adiabatic transfer pulse sequence and selected with pulsed field gradients. Skyline projections along both axes are shown.

samples acquired under identical conditions. Sample hydration was measured by TGA and corrected for. Only an approximately 1% error is introduced by the uncertainty regarding the nature of the extraframework aluminum (as measured by ^{29}Si MAS NMR at 9.4 T). The results of these analyses are presented in Table 1. In line with previous studies,[5,6,9,11] the 9.4 T single pulse experiment shows intensity from only 65% of the aluminum present, whereas the spin-echo experiment shows intensity from 85% of the aluminum present, suggesting that the broad resonance that is discriminated against in the single pulse experiment may account for the "invisible aluminum" reported in the literature.[3,6,8−12]

To probe the nature of the resonance, a MQMAS experiment was carried out at 9.4 T using field gradients for coherence selection and a RIACT excitation sequence (Figure 5). The S/N of the experiment is limited and the signals from higher aluminum coordinations are poor, but it is clear that two distinct tetrahedral environments are present: the maximum at 58 ppm in the 1D spectrum, assigned to tetrahedral framework aluminum, and another with a much larger quadrupolar coupling corresponding to the unresolved broad intensity distribution whose presence was suggested by the spin-echo spectra. Similar results have subsequently been obtained using the Bruker DSX 400 system with coherence selection by phase cycling.

The main difficulties in the further interpretation of these data arise from the limited resolution obtainable at 9.4 T, even employing fast spinning and also the nonquantitative nature of the experiments (Table 1). To some extent this is due to the

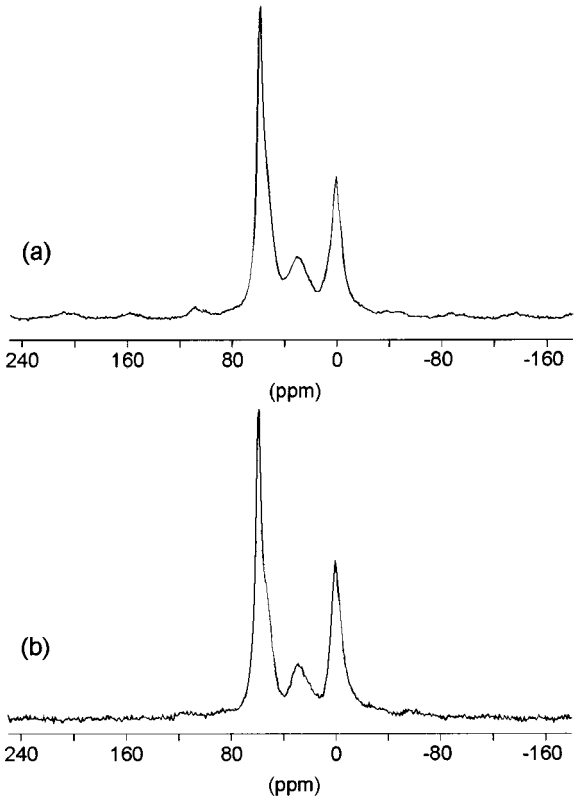

Figure 6. ^{27}Al MAS NMR spectra of USY at 208.43 MHz: (a) single pulse, 200 scans were acquired at a spinning rate of 10.2 kHz with a 100 ms recycle delay, and (b) 90−180° spin-echo, 2000 scans were acquired at a spinning rate of 11.9 kHz with a 500 ms recycle delay.

largely amorphous nature of the aluminum containing species (where distributions of chemical and quadrupolar shifts are to be expected) but a major contribution is from the residual quadrupolar interaction itself. Whatever its magnitude, this is inversely field dependent and both the interaction and the distribution of the interaction, introduced by distributions in local environments, should be reduced at higher magnetic field strengths. For this reason, experiments were carried out at 18.8 T (208.43 MHz, 800 MHz for ^{1}H) on a spectrometer made available to us at the Pacific Northwest National Laboratory, Richland, Washington. Figure 6 shows the ^{27}Al single pulse and spin-echo MAS spectra respectively at this field strength and can be compared directly with those of Figure 4. At 18.8 T the single pulse and spin-echo spectra are much more consistent with each other and both show intensity from ≥95% of the aluminum present (i.e. quantitative within the error limits of these data) indicating little discrimination between the different signals; quite different from the situation at 400 MHz. The small spinning sidebands observed are due to the approximate doubling of the chemical shift contribution in frequency units while the spinning rates are ≈10 kHz at both fields. The general resolution of the spectra is greatly improved and the intensity in the center of the spectrum greatly reduced. Three resonances are now clearly resolved at 61, 30, and 1 ppm with an additional broad resonance that appears as a distinct shoulder to high field of the tetrahedral resonance, at 54 ppm. Spin-echo measurements of T_2 confirm that this signal has a longer T_2 value than the sharp tetrahedral resonance and from spectra at long echo times it is estimated to cover a frequency range from 45 to 60 ppm with a maximum at ca. 54 ppm. This signal is considered to be due to the second tetrahedral aluminum species revealed by the MQMAS experiment at 400 MHz.

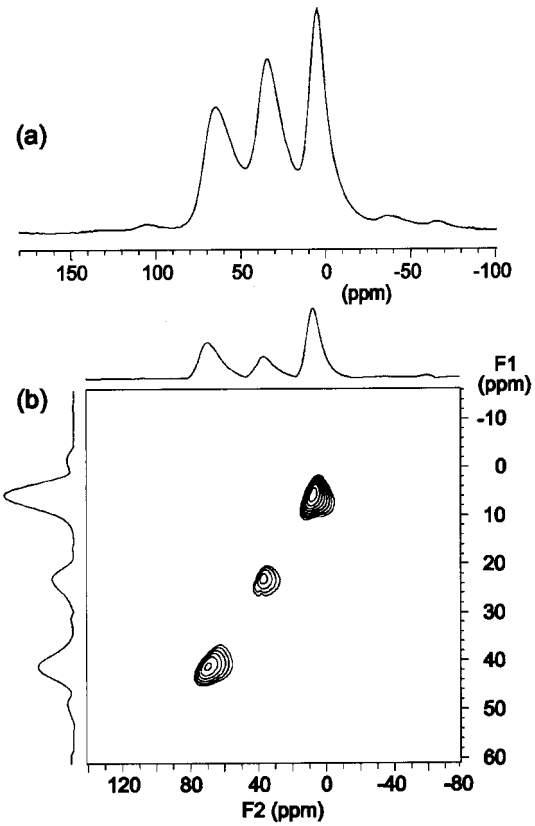

Figure 7. ^{27}Al NMR spectra of amorphous alumina gel[16] at 195.40 MHz: (a) 90−180° spin-echo, 2000 scans were acquired at a spinning rate of 13.7 kHz and a 200 ms recycle delay, and (b) MQMAS, recorded at a spinning rate of 15.1 kHz. Coherences were generated using a 2-pulse, nutation pulse sequence and selected with a 24-step phase cycle. A shearing transformation was performed after the first Fourier transform. Skyline projections along both axes are shown.

Further investigations of these four aluminum environments were carried out by MQMAS NMR at 18.8 T.

Before investigating the USY sample itself, experiments were carried out on a reference material to obtain benchmark spectral data on the behavior of the different aluminum coordinations in amorphous systems. Figure 7 shows the MAS and 2D MQMAS spectra of the amorphous alumina gel which contains substantial amounts of 4-, 5-, and 6-coordinate species. This was chosen because it contains all three proposed coordinations in amorphous environments but also because of the previously proposed similarities between such materials and the extraframework aluminum species in USY materials.[12] The spectra show well-defined broad resonances with maxima at 67, 35, and 6 ppm with slightly different line widths and small contributions from spinning sidebands. These are clearly reflected in the MQMAS spectrum, but while the 4 and 6 coordinations are observed with high S/N and in approximately the correct proportions, the contribution from the 5-coordinate aluminum is reduced. We have found this to be a general characteristic of MQMAS experiments on materials of these types under a variety of excitation schemes and conditions, with the RIACT sequence giving moderately better performance. The parameters derived from the fitting of the MAS spectra at 600 and 800 MHz are presented in Table 2.

Figure 8 shows the corresponding MQMAS experiment on the USY material at 800 MHz. In this case, there are four clearly resolved signals assigned to aluminum in tetrahedral (Al^{TET}), broad tetrahedral ($Al^{BR.TET}$), five-coordinate (Al^{PENT}), and octahedral (Al^{OCT}) environments. The signal intensity of the five-coordinate environment is discriminated against, as with the gel, but the signal in the 2D plot is clearly evident at 20 (F1) and 31 ppm (F2). This is in contrast to the low-field data where the 5-coordinate signal is not observed: a clear advantage of the use of high fields, particularly for samples of unknown structure.

Table 2. Summary of the Spectral Simulation Parameters for the Single Pulse ^{27}Al MAS Spectra of Amorphous Alumina Gel[a]

	δ_{CS}[b]/ppm	av C_Q[c]/kHz	η_Q[d]
Al^{TET}	65.2	655	0.3
Al^{PENT}	36.8	452	0.7
Al^{OCT}	1.9	535	0.0

[a] Chemical shift and quadrupolar coupling distributions are accounted for by an exponential broadening function with a chemical shift component proportional to the magnetic field strength and a quadrupolar coupling component inversely proportional to the magnetic field strength and a quadrupolar coupling component inversely proportianal to the magnetic field. [b] Isotropic chemical shift. [c] $C_Q = 3e^2qQ/2I^*(2I - 1)\hbar$. [d] The parameter η_Q has only a small effect on the simulated MAS spectrum.

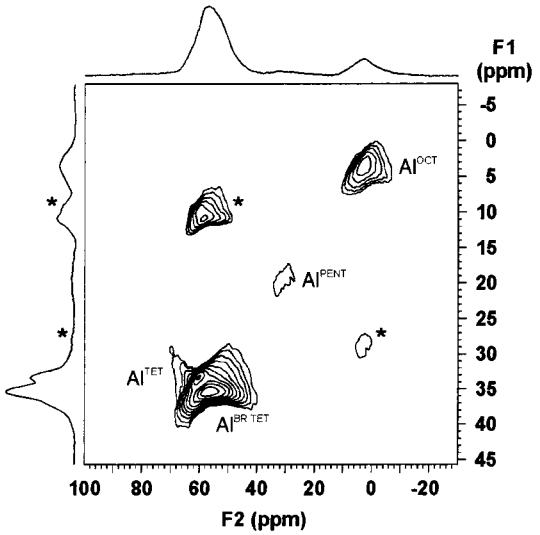

Figure 8. ^{27}Al MQMAS spectrum of USY at 208.43 MHz recorded at a spinning rate of 10.2 kHz. Coherences were generated using a 3-pulse, rotationally induced adiabatic transfer pulse sequence and selected with a 24-step phase cycle. A shearing transformation was performed after the first Fourier transform. Skyline projections along both axes are shown. Asterisks indicate spinning sidebands. Peak assignments are discussed in the text.

It is now possible to deduce the spectral parameters of all four sites, beginning with an interpretation of the 800 MHz ^{27}Al MAS NMR spectrum. The results are shown in Figure 9a with the fitting parameters given in Table 3. The resonance assigned to framework tetrahedral aluminum accounts for 33% of the total intensity. Framework Si/Al ratios of the Na-Y starting material (calculated from ^{29}Si MAS NMR) and of the USY sample (calculated both by ^{29}Si NMR and IR) also indicate that 33% of the aluminum remains in the USY framework following steaming. This suggests that the vast majority of the other aluminum species are extraframework in nature.

Confirmation of the accuracy of the analysis is given by the excellent agreement between the predicted and experimentally observed isotropic chemical shifts of the corresponding MQMAS spectra at both 800 and 400 MHz as shown in Table 4.

An even more challenging test is that the same fitting parameters from the analysis of the 800 MHz ^{27}Al MAS NMR spectrum should be able to correctly fit the lower field MAS spectra. The average parameters of the four aluminum environments used to simulate the ^{27}Al MAS NMR spectrum at 800

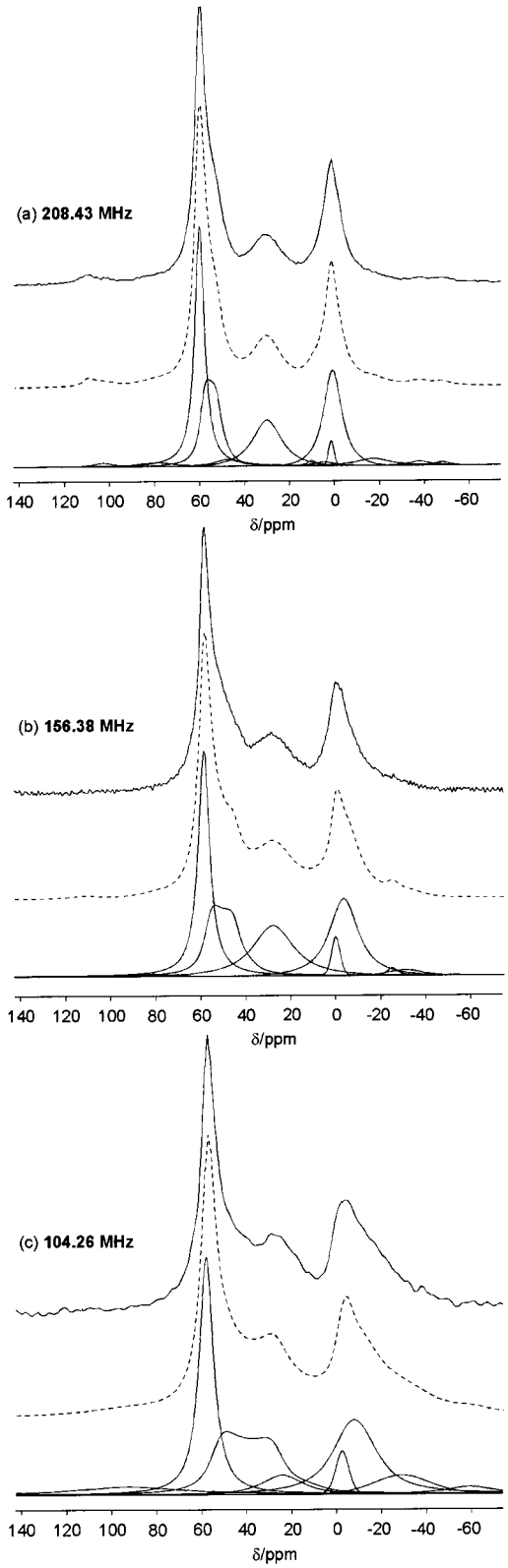

Figure 9. ^{27}Al single pulse MAS spectrum of USY at (a) 208.43, (b) 156.38, and (c) 104.26 MHz recorded at spinning rates of (a) 10.2, (b) 13.0, and (c) 9.8 kHz. Each spectrum is displayed above a simulation (dotted line) and a deconvolution of that spectrum. Spectral simulations and deconvolutions were made using "Dmfit 98".[17] Isotropic peaks are simulated by half-integer spin quadrupolar line shapes (parameters given in Table 3) with superimposed exponential broadenings. Spinning sideband intensities are approximated by peaks with mixed Lorentzian and Gaussian character.

Table 3. Summary of the Spectral Simulation Parameters for the Single Pulse ^{27}Al MAS Spectra of USY at 18.8 T[a]

	δ_{CS}[b]/ppm	av C_Q[c]/kHz	η_Q	% total intensity[d]
Al^{TET}	60.7	360	0.5	33
$Al^{BR.TET}$	60.4	940	0.1	21
Al^{PENT}	32.2	578	0.1[e]	20
Al^{OCT}	3.2	492	0.1[e]	26

[a] Chemical shift and quadrupolar coupling distributions are accounted for by an exponential broadening function with a chemical shift component proportional to the magnetic field strength and a quadrupolar coupling component inversely proportional to the magnetic field. [b] Isotropic chemical shift. [c] $C_Q = 3e^2qQ/2I(2I - 1)\hbar$. [d] Calculated to ±3% for 208.43 MHz spectrum using spinning sideband intensities approximated by line shapes with mixed Lorenzian and Gaussian character. [e] The parameter η_Q has a minimal effect on the simulated MAS spectrum (Figure 8a).

Table 4. Comparison of Experimental and Predicted 27Al MQMAS Isotropic (F1) Shifts of USY at 9.4 and 18.8 T[a]

	9.4 T		18.8 T	
	predicted	expt.	predicted	expt.
Al^{TET}	34.2	35.1	33.6	33.9
$Al^{BR.TET}$	40.2	42.7	35.0	35.8
Al^{PENT}	20.4		18.5	19.7
Al^{OCT}	3.8	−1.8	2.5	3.8

[a] Predicted shifts were calculated according to eq 11, Massiot et al.,[18] using the parameters given in Table 3.

MHz have been used to accurately simulate the ^{27}Al MAS NMR spectra of USY at both 400 and 600 MHz, as shown in Figure 9b,c. In these simulations, only the magnitudes of the four resonances were allowed to vary; the line shapes were determined from the parameters at 800 MHz and the known field dependencies of chemical shifts and second-order quadrupolar interactions. There is an excellent reproduction of all of the features of the spectra. The data in Table 3 indicate that the spectra at 600 and 800 MHz are in close agreement in terms of the intensities of the different resonances while those at 400 MHz are quite different, indicating that ^{27}Al measurements on these systems should be made at fields of 14 T or greater to ensure quantitative reliability. A similar conclusion has recently been drawn by Fitzgerald for ^{27}Al in various aluminas.[19]

Further general insight into the past difficulties in the interpretation of the lower field ^{27}Al MAS NMR spectra can be gained from an examination of the contributions of the individual resonances to the simulation of the 400 MHz ^{27}Al MAS spectrum. From Figure 9c it can be seen that the broad tetrahedral resonance has developed a clearly defined MAS quadrupolar line shape at 400 MHz. The high-field portion of the line shape overlaps with the resonance from the five-coordinate aluminum (which is now centered at 24 ppm) giving a composite "signal" observed at approximately 30 ppm, while the low-field portion of the line shape is overlapped with and obscured by the large tetrahedral resonance at 58 ppm. We have observed this overlap situation of tetrahedral and broad tetrahedral resonances to be a general feature of the ^{27}Al spectra of a variety of steamed HY materials. In this regard, the amorphous alumina gel studied in the present work may not be such a good model for the extraframework aluminum in the catalyst samples as has been suggested since its behavior is quite different both in the distributions and average quadrupolar and chemical shift parameters of the broad four- and five-coordinate aluminum environments (Tables 2 and 3). Such a situation might be expected; the pore and channel system dimensions of the zeolite framework may well place constraints on the geometries and sizes of any extraframework species within the lattice and they

may well be less random or amorphous than the gel materials and contain quite anisotropic local environments. The gels have been formed under conditions where there are comparatively greater opportunities for the relaxation of the local aluminum geometries.

Conclusions

All the ^{27}Al spectral simulations at the different field strengths and the tabulated data from the analyses reveal a consistent pattern of four clearly defined aluminium environments for this USY material (Table 3) and this is considered to be representative of this class of catalyst. Further, there are differences between the behaviors of these signals and those in the spectra of the amorphous alumina sample (Tables 2 and 3), indicating that amorphous materials of this type may be more limited as models for extraframework alumina than hoped.[16] This may be due to constraints imposed by the limited volumes available in the channel systems, which could restrict both the sizes and geometric arrangements in the oligomeric species produced during the dealumination resulting from steam treatment.

It is clear is that ^{27}Al MAS spectra at very high field strengths (at or close to 18.8 T) yield a sufficient degree of resolution for further magnetic resonance investigations of these materials to be rewarding. We are currently implementing coherence transfer connectivity experiments to unambiguously determine the locations of the different aluminum species contained in and within the frameworks and investigating the Lewis sites which they may support. It is probable that at high fields, MAS alone will be sufficient to achieve acceptable spectral resolution, greatly simplifying the experiments. It should be possible, in the longer term, to use these data to more clearly delineate any relationships between the different aluminum species present to the catalytic activities and selectivities of these materials. It may even be possible to obtain structure/reactivity relationships correlating the relative populations of the different aluminum environments with catalytic activities and product distributions as an aid in the further optimization of these catalysts.

Acknowledgment. This research was performed in the Environmental Molecular Sciences Laboratory (a national scientific user facility sponsored by the U.S. DOE Office of Biological and Environmental Research) located at the Pacific Northwest National Laboratory, operated by Battelle for the DOE. We would like to thank Dr. David Hoyt and the EMSL staff for their kind assistance and for access to their facility, without which this work would not have been possible. C.A.F. acknowledges the financial assistance of the NSERC of Canada in the form of operating and equipment grants.

JA003210K